SLAC-PUB-5859
July 1992
(A)

THE VERTICAL EMITTANCE IN THE ATF DAMPING RING*

T. O. RAUBENHEIMER
Stanford Linear Accelerator Center
Stanford University, Stanford, CA 94309

and

K. EGAWA, M. KIKUCHI, K. KUBO
S. KURODA, K. OIDE, S. SAKANAKA, N. TERUNUMA, J. URAKAWA
KEK, National Laboratory for High Energy Physics, Tsukuba, Ibaraki 305, Japan

Abstract

The results of calculations and simulations of the vertical emittance in the KEK Accelerator Test Facility damping ring are described. Both systematic and random alignment tolerances and a skew correction scheme are presented which limit the normalized vertical emittance to $\gamma\epsilon_y < 4.8 \times 10^{-8}$ m-rad. Finally, the effect of intrabeam scattering on the vertical emittance is calculated.

1. Introduction

In this paper, we will describe the results of calculations and simulations of the vertical emittance in the Accelerator Test Facility (ATF) damping ring being designed at KEK [1,2]. The ATF project is designed to test many of the technologies needed in a future linear collider. The project consists of an S-band electron injector, a damping ring, a bunch compressor, and finally, an X-band accelerator, and a final focus test. One of the more stringent requirements on a future linear collider is the generation and preservation

* Work supported in part by Department of Energy contract DE-AC03-76SF00515.

Submitted to Nuclear Instruments and Methods A.

of beams with very small emittances. Thus, one of the principal goals of the ATF damping ring is the generation of beams with normalized rms emittances of $\gamma\epsilon_x \leq 4 \times 10^{-6}$ m-rad and $\gamma\epsilon_y \leq 4.8 \times 10^{-8}$ m-rad. In this paper, we describe the results of calculations and simulations of the vertical emittance in the ATF damping ring and we present the tolerances required to achieve the desired emittance with a 95% confidence.

In a damping ring, the vertical emittance is primarily determined by the vertical dispersion and betatron coupling arising from alignment errors. We will calculate the random and systematic tolerances needed to achieve the design emittance and we will describe a skew quadrupole correction system designed to ease these tolerances. The calculations are performed using a mixture of analytic formulas and simulations; the analytic expressions provide insight into the sensitivities while the simulations are used to verify the results. Finally, we will briefly discuss the effect of intrabeam scattering on the vertical emittance; intrabeam scattering is a significant effect in this damping ring. We will not discuss any other current dependent effects, in general, they do not limit the vertical emittance [3], and we will not discuss the tolerances required to achieve the necessary beam position stability.

2. ATF Damping Ring

Before discussing the calculations, we need to briefly describe the ATF damping ring. The principal parameters of the ATF damping ring design are listed in table 1 and the lattice functions for half of the ring are plotted in figure 1. The ring consists of 36 FOBO cells where most of vertical focusing is provided by the combined function bending magnet located at the center of each cell. The ring is designed so that the horizontal phase advance per cell can be varied from 100° to 140°, varying the equilibrium horizontal emittance from

$\gamma\epsilon_x = 6.6 \times 10^{-6}$ m-rad to $\gamma\epsilon_x = 3.3 \times 10^{-6}$ m-rad; the parameters in table 1 correspond to the case where the cell phase advance is 130°.

The ring is designed in a racetrack form with two dispersion-free regions which contain the injection and extraction septa, the RF cavities, and 19.2 meters of damping wigglers which reduce the radiation damping rates by a factor of 2. The ring is designed to operate with a maximum current of 600 mA. Typically, it would damp multiple trains of bunches at once. The number of bunches per train varies from 10 to 60, depending on the single bunch charge, and the bunch-to-bunch separation is at least 1.4 ns; parameters listed in table 1 assume 20 bunches per train and 2×10^{10} particles per bunch.

3. Vertical Dispersion and Betatron Coupling

As mentioned, the vertical emittance in the ring is determined primarily by the vertical dispersion and the betatron coupling induced by alignment errors. In particular, vertical dipole errors and a non-zero vertical orbit in the quadrupoles will directly introduce vertical dispersion. Furthermore, a non-zero vertical closed orbit in the sextupoles, vertical sextupole misalignments, or quadrupole rotations will couple the horizontal and vertical planes. This coupling generates vertical dispersion by coupling to the horizontal dispersion and it couples the x and y betatron motion; higher-order effects, such as rotated sextupoles, are less important.

The contributions from the vertical dispersion and the betatron coupling to the vertical beam size and emittance have two components: one arises because the couplings increase the projection of the six-dimensional emittance in the vertical plane and the other arises from a fundamental increase in the vertical emittance. The first occurs because the couplings *locally* rotate the eigenvectors of the particle motion. Although the

projection of the beam is increased, the beam emittance is not changed. A simple example of this projection increase is the beam size due to vertical dispersion and a finite energy spread.

The second effect occurs because the noise due to the synchrotron radiation can couple into the vertical plane when the eigenvectors are rotated in the bending magnets. This leads to a growth of the vertical emittance. Here, the effect is not local; it depends upon the average of the coupling in all of the bending magnets. The important distinction between this effect and the former, is that the local rotations of the eigenvectors can be corrected even after the beam is extracted from the damping ring. In contrast, the increase in the beam emittance cannot be corrected after the beams are extracted; it must be reduced by correcting the sources of the coupling in the storage ring.

In the ATF damping ring we are primarily interested in the fundamental beam emittance, not in the local projected emittance; again, the local coupling can be corrected after the beam has been extracted. The emittance due to the vertical dispersion can be written [5]:

$$\gamma\epsilon_y = \frac{C_q\gamma^3}{\oint G^2 ds}\int_0^C ds\mathcal{H}_y(s)|G^3| \quad , \tag{1}$$

where we assumed that the vertical damping partition $\mathcal{J}_y$ equals one. In addition, $C_q = 3.84\text{-}\times 10^{-13}\,\mathrm{m}$, $G(s)$ is the inverse bending radius, and finally, $\mathcal{H}_y$ is the dispersion invariant:

$$\begin{aligned}\mathcal{H}_y(s) &= \gamma_y\eta_y^2 + 2\alpha_y\eta_y\eta_y' + \beta_y\eta_y'^2 \\ &= \frac{1}{4\beta_y\sin^2\pi\nu_y}\left|\int_s^{s+C} dz f(z)\sqrt{\beta_y}e^{i\left(\psi_y(s)-\psi_y(z)+\pi\nu_y\right)}\right|^2 \quad .\end{aligned} \tag{2}$$

Here, α_y, β_y, and γ_y are the twiss lattice parameters and the driving term f equals $f(z) =$

$y(K_2\eta_x - K_1) - \widetilde{K_1}\eta_x - G_y$ where K_1, $\widetilde{K_1}$, and K_2 are the normalized quadrupole, skew quadrupole, and sextupole magnetic field strengths and G_y is the inverse of the vertical bending radius.

Next, we can find a similar expression for the emittance contribution due to weak betatron coupling [4]:

$$\gamma\epsilon_y = \frac{C_q\gamma^3}{16\oint G^2 ds}\int_0^C ds\mathcal{H}_x|G^3|\left[\sum_{\pm}\frac{|Q_{\pm}(s)|^2}{\sin^2\pi\Delta\nu_{\pm}} + 2\mathrm{Re}\frac{Q_+^*(s)Q_-(s)}{\sin\pi\Delta\nu_+\sin\pi\Delta\nu_-}\right] \tag{3}$$

where

$$Q_{\pm}(s) = \int_s^{s+C} dz\tilde{k}(z)\sqrt{\beta_x\beta_y}e^{i\left[\left(\psi_x(s)\pm\psi_y(s)\right)-\left(\psi_x(z)\pm\psi_y(z)\right)+\pi(\nu_x\pm\nu_y)\right]} \quad . \tag{4}$$

Here, $\tilde{k} = (K_2 y - \widetilde{K_1})$ and the sum over $\pm$ denotes a sum over both the $+$ term (sum resonance) and the $-$ term (difference resonance) while $\Delta\nu_+ = \nu_x + \nu_y$ and $\Delta\nu_- = \nu_x - \nu_y$. In addition, the * is used to represent the complex conjugate and the operator "Re" yields the real portion of the expression. Finally, we should note that this definition of the coupling coefficient $Q_{\pm}$ is similar to the more common definitions [6] which are found from the fourier component at the sum and difference resonance, but equation (4) includes all harmonics and thus is a function of the azimuth s.

3.1 Random Alignment Errors

To calculate the effect of random errors, we can evaluate equations (1) and (3) assuming that the errors are uncorrelated. For the vertical sextupole misalignments y and

the quadrupole rotational errors Θ, we find expected values of the emittance:

$$\langle \gamma \epsilon_y \eta_y \rangle = \frac{\gamma \mathcal{J}_\epsilon \sigma_\epsilon^2}{4 \sin^2 \pi \nu_y} \left[4 \sum_{quad.} (K_1 L)^2 \eta_x^2 \beta_y \langle \Theta^2 \rangle + \sum_{sext.} (K_2 L)^2 \eta_x^2 \beta_y \langle y^2 \rangle \right]$$
$$\langle \gamma \epsilon_y \beta_\pm \rangle = \frac{\gamma \epsilon_x \mathcal{J}_x}{16 \sin^2 \pi \Delta \nu_\pm} \left[4 \sum_{quad.} (K_1 L)^2 \beta_x \beta_y \langle \Theta^2 \rangle + \sum_{sext.} (K_2 L)^2 \beta_x \beta_y \langle y^2 \rangle \right] \quad , \tag{5}$$

where we have used the expression for the rms energy spread σ_ϵ to simplify the expressions and we have neglected the cross-term in equation (3) since it is smaller by a factor of $1/2\pi\nu$.

Similar expressions for the effects of vertical quadrupole misalignments or rotations of the bending magnets are more complicated. These errors cause a non-zero closed orbit which is then corrected with the dipole corrector magnets. After orbit correction, the residual orbit depends upon the errors, the corrector placement, and the alignment of the Beam Position Monitors (BPMs). Furthermore, the closed orbit is correlated across many magnets and this leads to cancellations of the contributions. Thus, to estimate these effects, we will resort to simulations.

At this point, we can calculate the sensitivity of the various elements to random errors by calculating the normalized emittance assuming unit errors, $\langle \Theta^2 \rangle = \langle y^2 \rangle = 1$, and removing the tune dependence by multiplying by the resonant denominators: $\sin^2 \pi \nu_y$ and $\sin^2 \pi \Delta \nu_\pm$. We use equations (5) to calculate the effect of the vertical sextupole misalignments and the quadrupole rotations:

$$S_{\eta_y} = \frac{\gamma \mathcal{J}_\epsilon \sigma_\epsilon^2}{4} \left[4 \sum_{quad.} (K_1 L)^2 \eta_x^2 \beta_y + \sum_{sext.} (K_2 L)^2 \eta_x^2 \beta_y \right]$$
$$S_\beta = \frac{\gamma \epsilon_x \mathcal{J}_x}{16} \left[4 \sum_{quad.} (K_1 L)^2 \beta_x \beta_y + \sum_{sext.} (K_2 L)^2 \beta_x \beta_y \right] \quad , \tag{6}$$

and we estimate values for the bend rotations and the quadrupole misalignments by averaging the results of 100 simulations. In the simulations, the random errors are generated with gaussian distributions, cutoff at $\pm 2\sigma$, and the orbit is corrected in an rms sense with the dipole correctors.

The sensitivities to these angular and vertical misalignments are listed in tables 2 and 3. The values are separated into the dispersive and the betatron coupling contributions from the various magnet families; a value of $\gamma\epsilon_x = 3.65 \times 10^{-6}$ m-rad was used to calculate the betatron coupling contribution. Because the errors are random, the contributions are simply added to find the net effect. Notice that the contributions from the vertical dispersion are roughly one order of magnitude larger than the contributions due to the betatron coupling. Also notice that a few elements are very important, namely the arc focusing quadrupoles and the sextupoles, and thus extra attention should be given to these magnets.

At this point, we need to discuss the distribution of the emittance about the expected value. This is important because we wish to determine tolerances that will limit the vertical emittance with a high degree of confidence. In general, for given alignment tolerances, the value of the emittance that is exceeded in only 5% of the cases is two to three times larger than the expected value of the emittance [4]; the detailed value depends upon the tunes and the use of correction.

To estimate the magnitude of the alignment tolerances, we can use the results in tables 2 and 3 to calculate uniform tolerances. To limit the emittance to 4.8×10^{-8} m-rad with a 95% confidence, we want to strive for expected values of roughly 1.6×10^{-8} m-rad.

Thus, we find

$$\Theta_{\rm rms} \lesssim 550\,\mu{\rm rad}|\sin\pi\Delta\nu| \qquad y_{\rm rms} \lesssim 35\,\mu{\rm m}|\sin\pi\Delta\nu| \quad , \tag{7}$$

where the tolerances depend upon the choice of tunes. To ease the tolerances as much as possible, we need to restrict the operational tune space. Figure 2 is a plot of the tune diagram where we restricted $\Delta\nu_y > 0.17$, $\Delta\nu_\pm > 0.15$, and kept a reasonable distance from the horizontal integer and the half-integer resonances; resonance lines up to order of the normal sextupole resonances are included for guidance. The shaded regions are inaccessible.

These alignment tolerances and the accompanying restrictions on the tunes are fairly severe; they are smaller than 500 μrad and 30 μm which are thought to be the limits attainable in the ATF design. Fortunately, we will be able to ease the tolerances by roughly 50% with correction; we will describe the correction after discussing the effect of systematic errors.

3.2 Systematic Alignment Errors

In general, the systematic tolerances are looser than the random tolerances. This occurs because the phase advance in equations (1) and (3) leads to cancellation of the contribution. In a simple periodic system, the contribution from the systematic errors has the form:

$$({\rm systematic}) \propto \frac{1}{\sin^2(\pi\nu/N_p)\sin^2\pi\nu_c} \qquad \text{while} \qquad ({\rm random}) \propto \frac{N}{\sin^2\pi\nu} \quad . \tag{8}$$

Here, ν is the tune: $\nu_y, \nu_x \pm \nu_y$, N_p is the number of superperiods, N is the number of cells, and ν_c is the phase advance per cell: $\nu_{yc}, \nu_{xc} \pm \nu_{yc}$. Thus, provided that the tune per

superperiod is far from resonance and $\Delta\nu_c \gg 1/\pi\sqrt{N}$, the emittance is less sensitive to systematic errors than random errors; in the ATF ring, $\nu_c \approx 0.14$ while $1/\pi\sqrt{N} \approx 0.05$.

To compare with the random sensitivities listed in tables 2 and 3, we calculate the emittance contributions, assuming unit errors, at one of the possible working points for the ring, $\nu_x = 15.82$ and $\nu_y = 9.37$. These results are then scaled by $\sin^2 \pi\nu$ and are listed in tables 4 and 5. Of course, because the relationship on the tunes is more complex, these values are not independent of tunes as are the values in tables 2 and 3. Furthermore, unlike the random sensitivities, the individual contributions are not simply additive; the sum depends upon the relative phase of the contributions.

The individual systematic sensitivities are over a factor of five smaller than the random sensitivities, but we have to decide how to sum the contributions. If we assume the worst case, where all of the contributions are in phase, we find that the total is equal to the square of the sum of the square root of the individual terms: $(\text{total}) = \left[\sum \sqrt{(\text{individual})}\right]^2$. In contrast, if we assume that the relative phase between errors is random, we find that the expected value is simply equal to the sum of the separate values. The total sensitivity for both cases is listed in tables 4 and 5; the worst case values are roughly a factor of four worse than the random phase values.

Finally, to obtain a rough estimate of the tolerances, we note that in the worst case, the total sensitivity is a factor four less than the sensitivity to random errors, implying tolerances that are a factor of two looser than the random tolerances. In the other case, where we assumed random relative phases, the sensitivities are more than an order of magnitude smaller than the random sensitivities, implying tolerances that are a factor of three to four looser.

3.3 CORRECTION

In the ATF damping ring, the dominant contribution to the emittance is due to the dispersive errors. The vertical dispersion can be corrected with either skew quadrupoles in regions of horizontal dispersion or orbit bumps. Since we want to correct the dispersion without introducing betatron coupling, the ideal correctors are vertical orbit bumps in regions without sextupole magnets. Unfortunately, in the ATF, these regions are the wiggler and injection/extraction regions where the aperture may be limited. Thus, we will use skew quadrupoles in regions of horizontal dispersion. Alternately (and additionally), we could use orbit bumps in the arcs. Orbit bumps have the advantage of being more flexible than the fixed position skew quadrupoles but they have the disadvantage of being more complex to implement and possibly reducing the ring acceptance.

In theory, using two correctors, separated in phase by 90°, one could reduce the expected value of the emittance by a factor proportional to the resonant denominator: $2/3 \sin^2 \pi\nu_y$ [4]; additional correctors should provide further reductions. Note that the restrictions on the operating tune space are reduced because the resonant denominator is cancelled.

In simulations with $\nu_x = 15.82$ and $\nu_y = 9.37$, four skew quadrupoles, located for optimal tuning of both the vertical dispersion and the betatron coupling sum resonance (the closest coupling resonance), reduced the vertical emittance by a factor of three; this is slightly better than the factor $2/3 \sin^2 \pi\nu_y$. Further reduction of the dispersion is possible, but, at this level, the betatron coupling induced by the skew quadrupole correctors becomes significant.

Finally, it should be noted that to correct the dispersion, one needs to measure either

the beam emittance or the dispersion in the ring; ideally, one would do both. To limit the emittance contribution to $\gamma\epsilon_y \leq 4 \times 10^{-8}$ m-rad, we need to keep the rms dispersion at the level of 3 mm. Assuming a $\pm 1\%$ energy aperture, accurate measurements of the dispersion would require BPMs with a 15 μm precision (reading-to-reading jitter). This measurement should be readily achieved as the BPMs designed for the ATF ring have a 1.5 μm precision [7].

3.4 Tolerances

At this point, we can specify the tolerances needed to achieve the desired vertical emittance. We will specify systematic tolerances that are a factor of two looser than the random tolerances and we will assume that the relative phases of the systematic errors are random. To calculate the tolerances, we start from the sensitivities in tables 2–5, and divide by the resonant denominators. Next, to include the correction, we multiply these values by the correction factor: $2/3 \sin^2 \pi\nu$. Finally, to calculate the upper limit with a 95% confidence, we multiply by another factor which depends upon the tune and the correction. Curves can be found in ref. 4, but for the purpose of approximation, the factor is equal to 2.5 when the fractional tune is equal to 0.25 and it decreases to 2.1 when either the fractional tune approaches the half-integer or when correction is used.

Results are listed in tables 6 and 7 where we have calculated uniform tolerances with and without correction. The case without correction was calculated for tunes of $\nu_x = 15.66$ and $\nu_y = 9.17$; the tolerances could be eased by choosing the vertical tune closer to the half-integer. Both the expected values of the emittance and the 95% confidence level limit are listed. In addition, it is possible to calculate graded tolerances, where the sensitive elements have tighter tolerances; obviously the determination of the relative weighting

is a matter of choice. This has not been done since the uniform tolerances seem quite reasonable.

Finally, these tolerances have been compared with the results of 100 simulations without correction and 100 simulations where four skew quads were used to reduce the emittance. In the simulations, we use the tolerances listed in table 7 plus a random tolerance on the magnetic field strength of $\Delta B/B_{\rm rms} = 10^{-3}$. The random errors are found from gaussian distributions, cutoff at $\pm 2\sigma$, and the sign of the individual systematic errors was chosen randomly in each simulation. The tunes in the simulations were $\nu_x = 15.60$ and $\nu_y = 9.25$.

Without correction, the average emittance was found to be: $\langle \gamma \epsilon_y \rangle = 6.9 \times 10^{-8}$ m-rad and the 95% confidence maximum value is: $\gamma \epsilon_{y\,95\%} = 16.1 \times 10^{-8}$ m-rad; a histogram of the values found is plotted in figure 3(a). With correction, we found an average emittance: $\langle \gamma \epsilon_y \rangle = 2.3 \times 10^{-8}$ m-rad and the 95% confidence maximum value is: $\gamma \epsilon_{y\,95\%} = 4.8 \times 10^{-8}$ m-rad; a histogram of the emittance values is plotted in figure 3(b). These values are close to those calculated in table 7.

4. Intrabeam Scattering

When operating the ATF damping ring with large single-bunch currents, intrabeam scattering is expected to increase the beam emittance by a significant percentage. For example, with the parameters listed in table 1 and 2×10^{10} particles per bunch,intrabeam scattering increases the emittance by over 20%.

It is standard [8] to calculate the intrabeam scattering assuming that the emittance ratio ϵ_x/ϵ_y remains constant. This is valid when the vertical emittance is determined by

random coupling errors, but when the vertical emittance is determined by the vertical dispersion, this is no longer correct [3].

The reason can be simply understood by examining the emittance growth process. With intrabeam scattering, the prime mechanism for transverse emittance growth is similar to that of the synchrotron radiation. When two particles scatter, the longitudinal momentum can change and this is coupled into the transverse planes through the dispersion. The main difference between the growth due to the synchrotron radiation and that due to the intrabeam scattering, is that the radiation is only emitted in the bending magnets while the scattering occurs everywhere around the ring.

Thus, the intrabeam scattering emittance growth is proportional to

$$\Delta\epsilon_{y\,IBS} \propto \oint ds\mathcal{H}_x(s)|Q_{\pm}(s)|^2 \qquad \text{or} \qquad \Delta\epsilon_{y\,IBS} \propto \oint ds\mathcal{H}_y(s) \tag{9}$$

and

$$\Delta\epsilon_{x\,IBS} \propto \oint ds\mathcal{H}_x(s) \quad , \tag{10}$$

while the synchrotron radiation emittance is proportional to

$$\epsilon_y \propto \int_{bends} ds\mathcal{H}_x(s)|Q_{\pm}(s)|^2 \qquad \text{or} \qquad \epsilon_y \propto \int_{bends} ds\mathcal{H}_y(s) \tag{11}$$

and

$$\epsilon_x \propto \int_{bends} ds\mathcal{H}_x(s) \quad . \tag{12}$$

Both the betatron coupling and the vertical dispersion are due to errors and are random. Therefore, the expected values are independent of position and the average in the bending

magnets equals the average around the ring. But, the horizontal dispersion is not random; it is minimized in the bending magnets to reduce the horizontal emittance. Thus, we can express the ratios:

$$\begin{aligned} \frac{\Delta\epsilon_{x\,IBS}}{\epsilon_x} &= \frac{\Delta\epsilon_{y\,IBS}}{\epsilon_y} \qquad \text{(betatron coupling)} \\ \frac{\Delta\epsilon_{x\,IBS}}{\epsilon_x} &> \frac{\Delta\epsilon_{y\,IBS}}{\epsilon_y} \qquad \text{(vertical dispersion)} \quad . \end{aligned} \tag{13}$$

The difference between the horizontal and vertical ratios, with vertical dispersion, depends upon the average of $\mathcal{H}_x$ around the ring relative to the average in the bending magnets.

In the ATF damping ring, the vertical emittance is determined primarily by the vertical dispersion and thus we can expect intrabeam scattering to have a smaller relative growth in the vertical than in the horizontal. To calculate this, we modified the formalism of Bjorken and Mtingwa [9] to include the vertical dispersion and the weak betatron coupling as specified by $Q_{\pm}(s)$; a more exact formalism for the intrabeam scattering with linear coupling is given in ref. 10. This calculation was performed after each of the 200 simulations described in section 3.4 with a charge per bunch of $2 \times 10^{10}\ e^-$; the results are listed in table 8. In the cases without correction, we see that the intrabeam scattering increases the horizontal emittance 5 times more than the vertical. After correction of the vertical dispersion, this ratio drops to a factor of 2.5.

5. Discussion

We have calculated the random and systematic alignment tolerances needed to achieve a normalized vertical emittance less than $\gamma\epsilon_y < 4.8 \times 10^{-8}$ m-rad in the ATF damping ring. Without any skew correction, the tolerances and the restrictions on the operating tune space are tight. The rms tolerances are $y_{\rm rms} \leq 17\,\mu$m and $\Theta_{\rm rms} \leq 300\,\mu$rad with systematic tolerances twice these values.

These tolerances can be eased substantially with simple correction. There are two reasons for this: first, the correction decreases the expected value, and, second, it also decreases the deviations about the expected value. With four skew quadrupoles in regions of dispersion, random and systematic tolerances of $y_{\rm rms} \leq 50\,\mu$m, $y_{\rm sys} \leq 100\,\mu$m, $\Theta_{\rm rms} \leq 500\,\mu$rad, and $\Theta_{\rm sys} \leq 1$ mrad will yield a vertical emittance less than 4.8×10^{-8} m-rad with a 95% confidence; the expected value is roughly a factor of two smaller.

The ATF alignment system is actually being designed to achieve random tolerances of $y_{\rm rms} = 30\,\mu$m and $\Theta_{\rm rms} = 500\,\mu$rad. In this case, we would expect a vertical emittance less than $\gamma\epsilon_y < 3.4 \times 10^{-8}$ m-rad with a 95% confidence; further reductions will likely be possible with additional correction using orbit bumps.

We have also calculated the intrabeam scattering contribution to the vertical emittance. We find that the growth due to the scattering of the vertical emittance is less than half of the growth of the horizontal emittance. This occurs because the vertical emittance is determined by the vertical dispersion and not the betatron coupling.

Finally, we should note that we have calculated the fundamental emittance and not the full projected emittance which also includes contributions from the local couplings. In theory, these local effects can be removed after the beam is extracted from the damping

ring. Assuming that the vertical emittance in determined by the vertical dispersion, the local couplings will increase the expected value of the projected emittance by roughly 25%; if the emittance is determined by the betatron coupling, the local couplings would double the expected value of the projected emittance.

Acknowledgements

I (TR) would like to thank my hosts at KEK for the opportunity to participate in this very interesting project and for their generous hospitality during my visit.

References

1. J. Urakawa, "Accelerator Test Facility (ATF)," *Proceedings of the Second Workshop on the Japan Linear Collider (JLC)*, KEK Proceedings 91–10 (1991).

2. S. Kuroda, *et al.*, "Damping Ring of ATF," *Proceedings of the Second Workshop on the Japan Linear Collider (JLC)*, KEK Proceedings 91–10 (1991).

3. T. O. Raubenheimer, "The Generation and Acceleration of Low Emittance Flat Beams for Future Linear Colliders," Ph.D. thesis, Stanford University, SLAC–Report–387 (1991).

4. T. O. Raubenheimer, "Tolerances to Limit the Vertical Emittance in Future Storage Rings," *Particle Accelerators*, **36** (1991) 75–119 .

5. M. Sands, "The Physics of Electron Storage Rings," SLAC–121 (1971).

6. For example see: A. W. Chao and M. J. Lee, "Particle Distribution Parameters in an Electron Storage Ring," *J. App. Phys.*, **47** (1976) 4453; G. Guignard, "Betatron Coupling with Radiation," *Proc. of the 1985 CERN Advanced Acc, School,* CERN 87–03 (1987).

7. M. Tejima, "BPMs for the ATF," to be published in KEK proceedings.

8. For example, the computer codes SAD or ZAP.

9. J. D. Bjorken and S. K. Mtingwa, "Intrabeam Scattering," *Particle Accelerators*, **13** (1983) 115.

10. A. Piwinski, "Intrabeam Scattering in the Presence of Linear Coupling," DESY 90–113 (1990).

Table 1. Parameters of the ATF damping ring.

Energy	1.54 GeV
Circumference	138.6 meters
Lattice	FOBO with CF bends
Damping part. $\mathcal{J}_x$	1.31
Current	600 mA maximum
$\gamma\epsilon_x$ w/o IBS	3.65×10^{-6} m-rad
$\gamma\epsilon_x$ w/ IBS (2×10^{10}/bunch)	4.39×10^{-6} m-rad
$\sigma_z, \sigma_\epsilon$ w/ IBS	5.2 mm, 0.81×10^{-3}

Table 2. Sensitivities to random angular misalignments.

	Num.	$S_{\eta_y}(\Theta)[10^{-3}\,\mathrm{rad}^{-2}\cdot\,\mathrm{m\text{-}rad}]$	$S_{\beta}(\Theta)[10^{-3}\,\mathrm{rad}^{-2}\cdot\,\mathrm{m\text{-}rad}]$
Bend (dipole field)	36	4.81 ± 0.42	0.29 ± 0.08
Bend (quad field)	36	2.65	0.24
Arc QFs	26	7.25	0.46
Matching Quads	40	3.20	0.45
Insertion Quads	18	1.90	0.47
Total	–	19.81	1.91

Table 3. Sensitivities to random vertical misalignments.

	Num.	$S_{\eta_y}(y)[\mathrm{m}^{-2} \cdot \text{m-rad}]$	$S_\beta(y)[\mathrm{m}^{-2} \cdot \text{m-rad}]$
BPMs	60	0.66 ± 0.04	0.17 ± 0.04
Arc QFs	26	0.82 ± 0.11	0.22 ± 0.01
Matching Quads	40	0.43 ± 0.04	0.08 ± 0.00
Insertion Quads	18	0.15 ± 0.01	0.01 ± 0.00
SF	32	1.60	0.19
SD	34	2.75	0.15
Total	–	6.41	0.82

Table 4. Sensitivities to systematic angular misalignments.

	Num.	$S_{\eta_y}(\Theta)[10^{-3}\,\mathrm{rad}^{-2}\cdot\,\mathrm{m\text{-}rad}]$	$S_{\beta}(\Theta)[10^{-3}\,\mathrm{rad}^{-2}\cdot\,\mathrm{m\text{-}rad}]$
Bends	36	0.71	0.14
Arc QFs	26	0.36	0.09
Matching Quads	40	0.21	0.04
Insertion Quads	18	0.18	0.03
Total (worst case)	–	7.13	1.43
Total (random)	–	1.46	0.30

Table 5. Sensitivities to systematic vertical misalignments.

	Num.	$S_{\eta_y}(y)[\mathrm{m}^{-2} \cdot \mathrm{m\text{-}rad}]$	$S_\beta(y)[\mathrm{m}^{-2} \cdot \mathrm{m\text{-}rad}]$
BPMs	60	0.07	0.03
Arc QFs	26	0.00	0.00
Matching Quads	40	0.01	0.00
Insertion Quads	18	0.02	0.01
SF	32	0.11	0.05
SD	34	0.21	0.05
Total (worst case)	–	1.70	0.67
Total (random)	–	0.42	0.15

Table 6. Uniform tolerances without correction; the tunes are assumed to be $\nu_x = 15.66$ and $\nu_y = 9.17$.

Tolerance	$\langle\gamma\epsilon_y\rangle[10^{-8}$ m-rad]	$\gamma\epsilon_{y\,95\%}[10^{-8}$ m-rad]
$\Theta_{\rm rms} = 250\,\mu$rad	0.5	1.4
$\Theta_{\rm sys} = 500\,\mu$rad	0.2	0.5
$y_{\rm rms} = 17\,\mu$m	0.8	2.2
$y_{\rm sys} = 34\,\mu$m	0.3	0.7
Total	1.8	4.8

Table 7. Uniform tolerances with correction.

Tolerance	$\langle\gamma\epsilon_y\rangle[10^{-8}$ m-rad]	$\gamma\epsilon_{y\,95\%}[10^{-8}$ m-rad]
$\Theta_{\rm rms} = 500\,\mu$rad	0.3	0.7
$\Theta_{\rm sys} = 1$ mrad	0.2	0.3
$y_{\rm rms} = 50\,\mu$m	1.2	2.6
$y_{\rm sys} = 100\,\mu$m	0.4	0.9
Total	2.1	4.5

Table 8. Intrabeam scattering before and after correction of the vertical emittance.

	$\Delta\epsilon_x/\epsilon_x$	$\Delta\epsilon_y/\epsilon_y$
Before correction	53%	11%
After correction	42%	17%

Figure Captions

1. Lattice parameters of half of the ATF damping ring.

2. Tune space with restrictions due to coupling.

3. Emittance values from simulations (a) with no skew correction and (b) with 4 skew quad correctors.

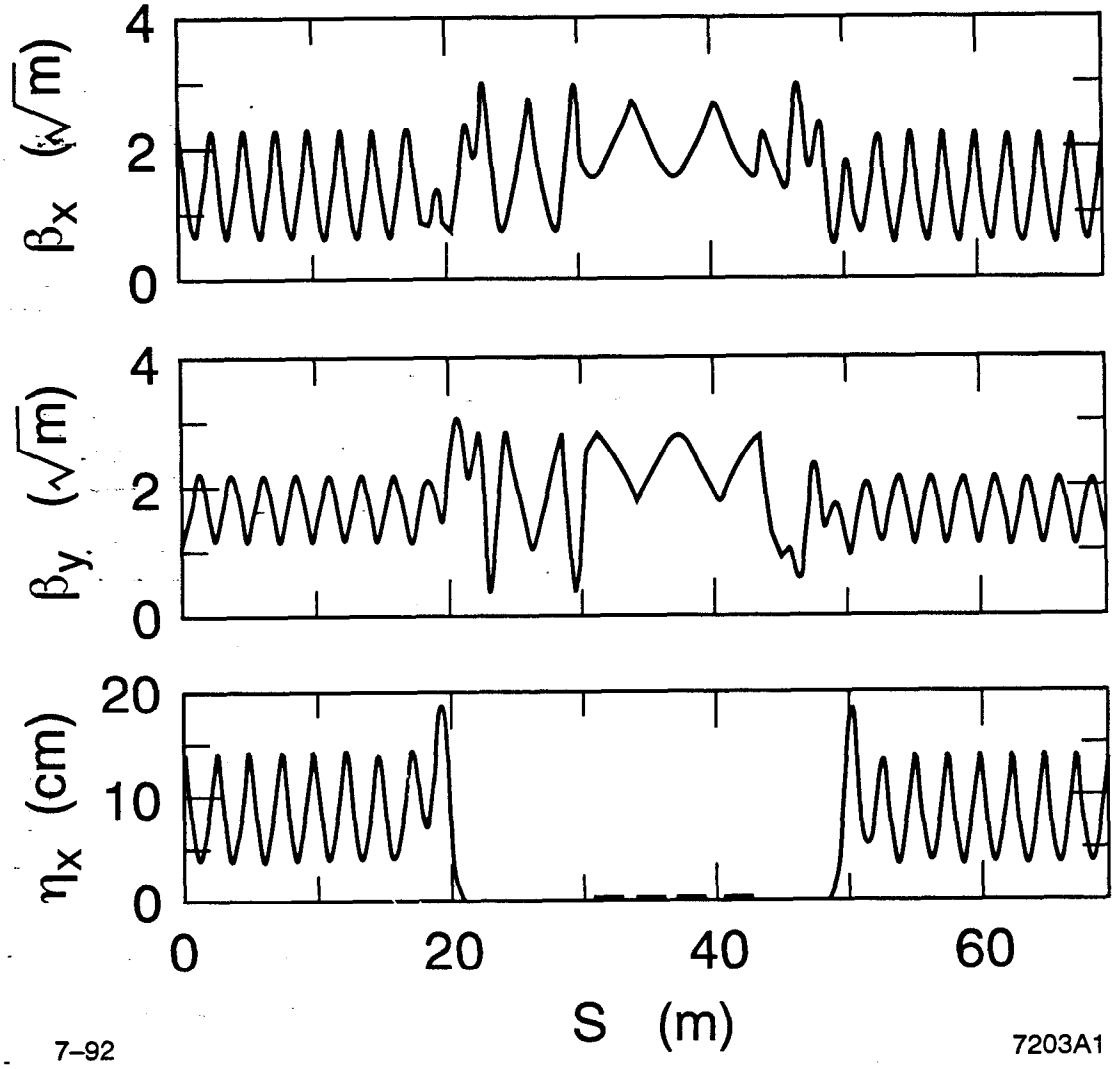
4
2
0
β_x ($\sqrt{m}$)
4
2
0
β_y ($\sqrt{m}$)
20
10
0
η_x (cm)
0
20
40
60
S (m)
7–92
7203A1

Fig. 1

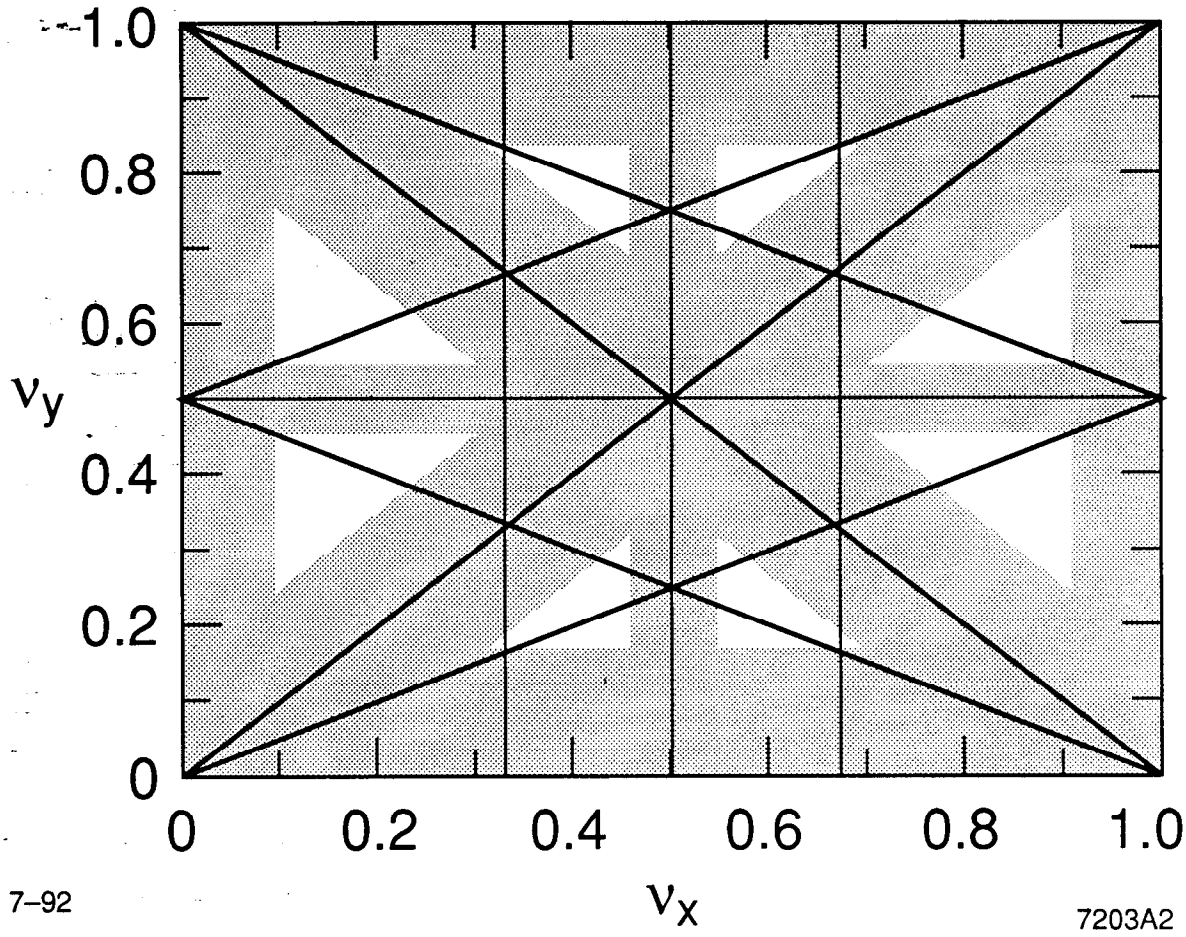

Fig. 2

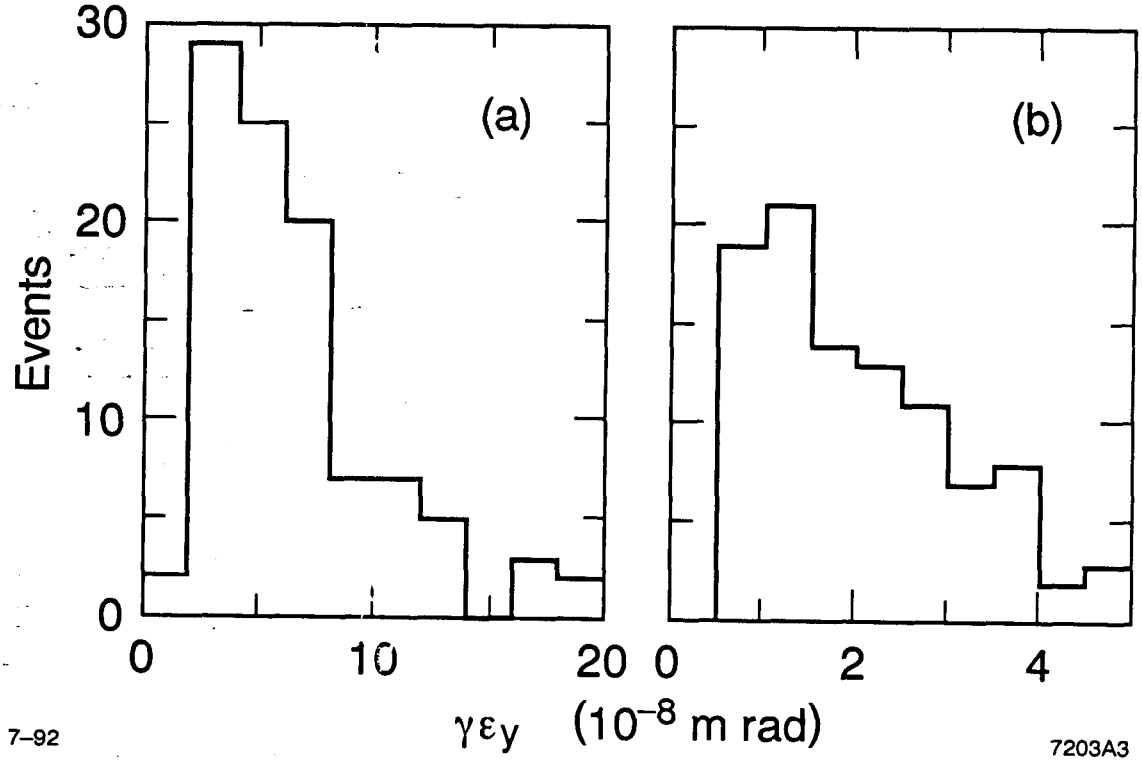

Fig. 3